Upconversion luminescence of Y_2O_3:Er^{3+}, Yb^{3+} nanoparticles prepared by a homogeneous precipitation method

LI Yanhong (李艳红)[1], ZHANG Yongming (张永明)[1], HONG Guangyan (洪广言)[2], YU Yingning (于英宁)[2]

(1. School of Material Science and Engineering, Shenyang Institute of Chemical Technology, Shenyang 110142, China; 2. Key Laboratory of Rare Earth Chemistry and Physics, Chinese Academy of Sciences, Changchun 130022, China)

Abstract: Y_2O_3: Er^{3+}, Yb^{3+} nanoparticles were synthesized by a homogeneous precipitation method without and with different concentrations of EDTA 2Na. Upconversion luminescence spectra of the samples were studied under 980 nm laser excitation. The results of XRD showed that the obtained Y_2O_3:Er^{3+},Yb^{3+} nanoparticles were of a cubic structure. The average crystallite sizes calculated were in the range of 28–40 nm. Green and red upconversion emission were observed, and attributed to $^2H_{11/2}$,$^4S_{3/2} \rightarrow {}^4I_{15/2}$ and $^4F_{9/2} \rightarrow {}^4I_{15/2}$ transitions of the Er^{3+} ion, respectively. The ratio of the intensity of green emission to that of red emission drastically changed with a change in the EDTA 2Na concentration. In the sample synthesized without EDTA, the relative intensity of the green emission was weaker than that of the red emission. The relative intensities of green emission increased with the increased amount of EDTA 2Na used. The possible upconversion luminescence mechanisms were discussed.

Keywords: homogeneous precipitation method; Y_2O_3: Er^{3+}, Yb^{3+} nanoparticles; upconversion luminescence; rare earths

It is well known that rare earth doped Y_2O_3 has extensive application in optical display and light emitting devices[1,2]. Considerable interest has been devoted to upconversion luminescence on account of potential applications to solid-state lasers, displays, fiber amplifiers and assay of biological compounds[3–5]. Y_2O_3 has been a promising host material owing to better chemical durability, thermal stability as well lower phonon energy[6,7].

On the other hand, nanoparticles have been studied vigorously over the past years on account of their potential applications and for the requirement of basic science research. In particular, nanometer-sized upconversion luminescence can be used as a labeling material for immunoassays and DNA assays[8]. Upconversion materials of rare earth doped Y_2O_3 have been synthesized by a variety of methods including the sol-gel method[9], hydrothermal method[10], combustion process[11], and so on. The conventional urea homogeneous precipitation method[12] is used because it is a simple, inexpensive and fast. In addition, appropriate complex agents are sometimes used. However, a precipitation medium is an important factor in the precipitation process, which can influence the microstructure, and results in the change of the upconversion luminescence property. So far, there are few reports on the effect of the complex on structures and upconversion emission properties.

In this article, nanocrystalline Y_2O_3: Er^{3+}, Yb^{3+} phosphors were prepared by the urea homogeneous precipitation method, with EDTA 2Na as a complex agent. The authors studied the effect of the amount of EDTA 2Na used on structures and upconversion luminescence properties.

1 Experimental

$Y(NO_3)_3$, $Yb(NO_3)_3$, and $Er(NO_3)_3$ stock solution (0.05 mol/L) was prepared by dissolving Y_2O_3, Yb_2O_3 and Er_2O_3 in dilute HNO_3, respectively, until the powders were all dissolved. Subsequently the excess acid was allowed to evaporate. After cooling to room temperature, deionized water was added, and 1 mol/L urea solution and 0.05 mol/L EDTA 2Na were prepared by dissolving the appropriate amount of urea and EDTA 2Na in deionized water.

Nanocrystalline Y_2O_3:Er^{3+}, Yb^{3+} samples were synthesized by the urea homogeneous precipitation method with a varying concentration of EDTA 2Na. The nitrate solutions containing Y $(NO_3)_3$ (77 ml), $Yb(NO_3)_3$ (20 ml), $Er(NO_3)_3$ (3 ml) and urea solution (120 ml) were mixed. Next, EDTA 2Na (the amounts were 0, 50, 75 ml) was added to the mixture solution, respectively. Uniform mixture solutions were

formed with stirring. The mixtures were heated at 90 °C for 3 h in a water bath. The precipitations were obtained by filtering and washed twice with deionized water, which were subsequently dried at 60 °C to obtain precursor powders. Finally, the precursor powders were fired in air at 850 °C for 2 h to get the corresponding nanocrystalline Y$_2$O$_3$:Er^{3+}, Yb^{3+}, respectively. The samples were marked a, b, and c, according to the amount of EDTA 2Na used being 0, 50, and 75 ml respectively (the molar ratio of EDTA 2Na to metal ions is 0, 0.5 and 0.75, respectively).

X-ray powder diffraction patterns were recorded with a Rigaku D/max IIB X-ray powder diffractometer with Cu Kα (λ=0.15406 nm) radiation. The morphology was investigated with the help of a Philips XL30 ESEM ODP field emission scanning electron microscope (SEM). The energy dispersive X-ray (EDX) spectrum of the Y$_2$O$_3$:Er^{3+}, Yb^{3+} samples were obtained using this instrument. The upconversion emission spectra of all samples were excited using Continuum Sunlite EX OPO, pumped by a Continuum Precision II Nd:YAG laser, and the output wavelength was 980 nm, the upconvert fluorescent light was dispersed with an Acton Spectra Pro-2758 spectrograph and detected with a nitrogen-cooled CCD camera (LN/CCD-1100 PB/UVAR). Luminescence spectra were recorded by averaging the emission over at least 10 excitation pulses. All of the measurements were carried out at room temperature.

2 Results and discussion

2.1 Structure of Y$_2$O$_3$: Er^{3+}, Yb^{3+}

Fig.1 shows the X-Ray powder diffraction patterns of the Y$_2$O$_3$: Eu^{3+}, Yb^{3+} samples, synthesized. All the samples exhibit identical diffraction patterns, which are well consistent with JCPDS No.43-1036 and confirm that the samples are of
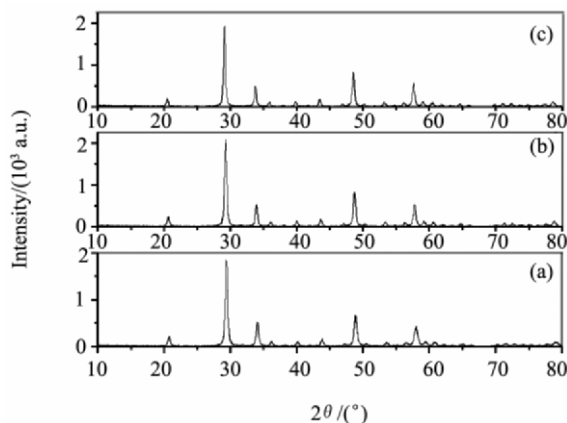

Fig.1 XRD patterns of the Y$_2$O$_3$:Er^{3+}, Yb^{3+} nanoparticles
Molar ratio of EDTA 2Na to metal ions is: (a) 0, (b) 0.5 and (c) 0.75

cubic structure with space group Ia3 (206). By applying the Scherrer formula to the full width at half maximum of the (222) diffraction peaks, the mean particle sizes have been calculated as 28, 34, and 40 nm for samples a, b, and c, respectively. In addition, the refined crystallographic unit cell parameters have been obtained with jade analysis software. The lattice constant, cell volume and calculated crystallite sizes are listed in Table 1. It is concluded that the unit cell parameters and the average crystallite sizes are related to the preparation condition. Moreover, the lattice constants and cell volumes obtained increase with increasing amount of EDTA 2Na used as a complex. These are results from less Yb^{3+} ions doping into Y$_2$O$_3$: Er^{3+}.

Fig.2 shows the SEM photograph of Y$_2$O$_3$:Eu^{3+}, Yb^{3+} nanocrystals whose precursors were prepared without and with a different amount of EDTA 2Na. The microphotographs of the samples show spherical morphology. All the particle sizes are similar and around 100 nm. This means that the particles are an aggregate of nanocrystals. The dispersion of the sample synthesized without EDTA 2Na is better than that with EDTA 2Na. The connected particles for sample b and c are on account of the hydrogen bond between precipitations and EDTA 2Na, when EDTA 2Na is present[13].

Fig.3 shows the EDX spectra, which display the chemical composition of all the samples, which is mostly Y, O, Yb, and Er. However, an obvious difference is observed in the samples prepared without and with EDTA 2Na. Minor amounts of Yb^{3+} ions are exhibited in the samples prepared with EDTA 2Na, which are related to the synthesis process. In the synthesis system of Re(NO$_3$)$_3$, urea and EDTA 2Na, Re-EDTA complex between EDTA and RE^{3+} ions are formed prior to the formation of Re(OH)CO$_3$ at room temperature. However, with heating at 90℃ in a water bath, the Re(OH)CO$_3$ precipitates appear with OH$^-$ ions released on account of the hydrolysis of urea. Because the order of complex ability of rare earth ions with EDTA is Yb^{3+} ions>Er^{3+} ions, there is a concentration deviation of Yb^{3+} ions in the precipitations because of the EDTA 2Na used. Higher and lower concentrations of Yb^{3+} exist in precipitations without and with EDTA 2Na, respectively, which remain in Y$_2$O$_3$:Er^{3+},Yb^{3+} nanoparticles after they are fired.

Table 1 Lattice constant, cell volume and crystallite size calculated for Y$_2$O$_3$: Er^{3+} and Y$_2$O$_3$: Er^{3+}, Yb^{3+}

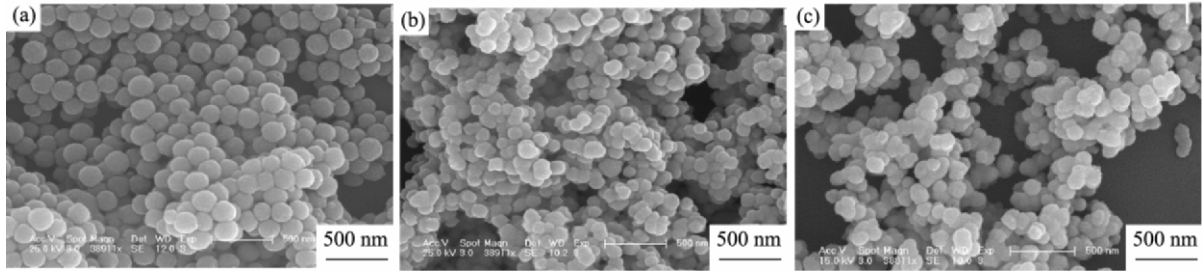| Samples	Lattice constant /nm	Cell volume/nm^3	Crystallite size/nm
JCPDS 41-1036	1.0604	1.1924	
A	1.0524±0.0005	1.1656	28
B	1.0569±0.00024	1.1804	34
C	1.0604±0.00006	1.1925	40

Fig.2 SEM image of the Y_2O_3: Er^{3+}, Yb^{3+} nanoparticles

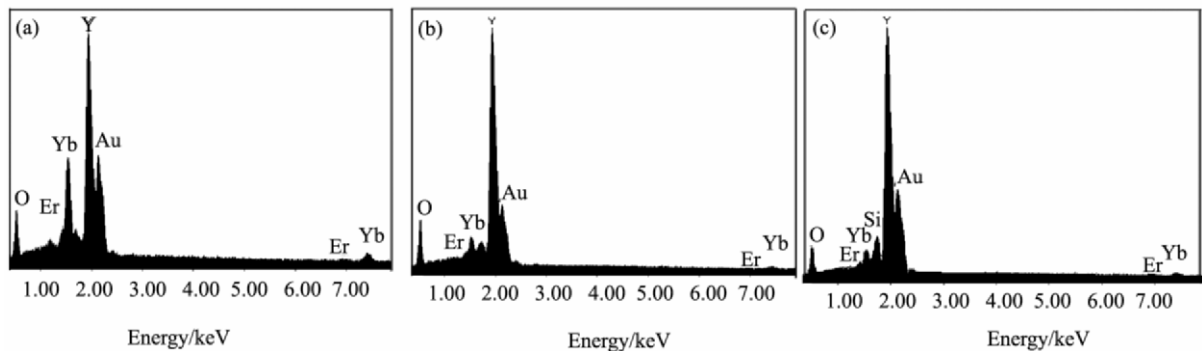Molar ratio of EDTA 2Na to metal ions is 0 (a) Sample a, 0.5 (b) Sample b and 0.75 (c) Sample c

Fig.3 EDX spectra of the Y_2O_3: Er^{3+}, Yb^{3+} nanoparticles

Molar ratio of EDTA 2Na to metal ions is (a) 0, (b) 0.5 and (c) 0.75

2.2 Upconversion luminescence properties of Y_2O_3: Er^{3+}, Yb^{3+} nanocrystals

The upconversion luminescence spectra of Y_2O_3:Er^{3+}, Yb^{3+} nanoparticles prepared without and with a varying concentration of EDTA 2Na under 980 nm laser excitation are shown in Fig.4. There are two upconversion emission bands corresponding to the green emission around 546–563 nm and the red emission around 652-683 nm, which are associated with the $^2H_{11/2}$, $^4S_{3/2} \rightarrow ^4I_{15/2}$ transition and the $^4F_{9/2} \rightarrow ^4I_{15/2}$ transition of Er^{3+} ions[14], respectively. It is observed that the relative emission intensities of green to red depend strongly on the amount of EDTA 2Na used as a complex. For the sample synthesized without EDTA (Sample a), the intensity of the green emission is weaker than that of the red emission. However, the intensity of green emission increases with an increased amount of EDTA 2Na used.

Fig.5 shows a typical energy level diagram for the upconversion emission of Yb^{3+}/Er^{3+} codoped materials under 980 nm infrared excitation[15,16]. The dominant upconversion mechanisms are energy transfer upconversions (ET) and excited state absorptions (ESA) in Er^{3+} and Yb^{3+} codoped systems. The mechanism for ESA is comparatively simple. The 980 nm excite light directly excites the Er^{3+} ion from the ground-state $^4I_{15/2}$ to the excited state $^4I_{11/2}$. Subsequently, a second photon from the laser source promotes the ion to the

$^4F_{7/2}$ level. The $^4F_{7/2}$ state decays nonradiatively to the $^2H_{11/2}$, $^4S_{3/2}$ and $^4F_{9/2}$ levels. In addition, the Er^{3+} ions on the excited state $^4I_{11/2}$ decay nonradiatively to the $^4I_{13/2}$ and are excited to the $^4F_{9/2}$ level by absorbing the second 980 nm photon energy. As for the mechanism for ET, because Yb^{3+} ions have a much larger absorption cross section relative to that of the Er^{3+} ions around 980 nm, an Er^{3+} ion is excited from the ground-state $^4I_{15/2}$ to the excited state $^4I_{11/2}$ by energy transfer from the excited Yb^{3+} ion, which is subsequently
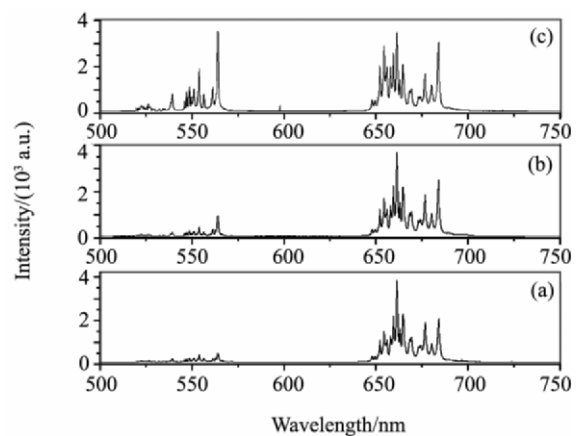

Fig.4 Upconversion luminescence spectra of Y_2O_3:Er^{3+}, Yb^{3+} nanoparticles

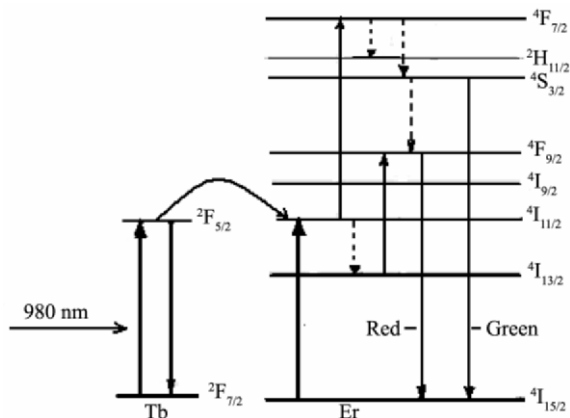Molar ratio of EDTA 2Na to metal ions is: (a) 0, (b) 0.5 and (c) 0.75

Fig.5 Energy level diagram for the upconversion emission of Yb^{3+}/Er^{3+} materials under 980 nm infrared excitation

excited to the $^4F_{7/2}$ state of the Er^{3+} ion by absorbing another Yb^{3+} energy. The green and red emissions were observed from the $^2H_{11/2}$, $^4S_{3/2} \rightarrow {}^4I_{15/2}$ and $^4F_{9/2} \rightarrow {}^4I_{15/2}$ transitions of Er^{3+} ions.

In the Er^{3+} and Yb^{3+} ion codoped systems, the energy transfer process (ET) is preponderant when compared with the excited state absorption (ESA). These energy transfer processes are strongly dependent on the codoping ion concentration. It was observed that green emission is much weaker in the sample synthesized without EDTA, on account of higher the Yb^{3+} concentration in the sample. Based on reported studies[6,7,15], the energy transfer process, $^4F_{7/2}$ $(Er) + {}^4F_{7/2}$ $(Yb) \rightarrow {}^4I_{11/2}$ $(Er) + {}^4F_{5/2}$ (Yb), depopulates the excited $^4F_{7/2}$ level and causes a decrease in green emission intensity. However, it must also be noted that the relative intensity ratio of green to red varies with the amount of EDTA used. As shown in Fig.3, the two samples possess similar Yb^{3+} ion concentration, therefore, another effect should be considered. Generally, increase in hychoxyl and carbonates for the sample with smaller crystallite size(sample b) is helpful to increase the nonradiative relaxation process, $^4I_{11/2}$ $(Er) \rightarrow {}^4I_{13/2}$ (Er)[8], which decreases Er^{3+} ions interacting in energy transfer, $^4F_{11/2}(Er) + {}^4F_{11/2}$ $(Er) \rightarrow {}^4I_{7/2}$ $(Er) + {}^4F_{15/2}$ (Er), as a result, the green emission is inferior on account of less Er^{3+} ions on $^2H_{11/2}$ and $^4S_{3/2}$ level.

3   Conclusion

Y_2O_3:Er^{3+}, Yb^{3+} nanoparticles were synthesized by a homogeneous precipitation method with EDTA 2Na of different concentrations, and upconversion luminescence spectra were studied under 980 nm laser excitation. The results of XRD showed that two samples were of a cubic structure. The average crystallite sizes were calculated as 28, 34 and 40 nm for the sample without and with different concentrations of EDTA 2Na respectively. The lattice constants and cell volumes increase with increasing amount of EDTA 2Na used as a complex, which results from less Yb^{3+} ions doping into Y_2O_3: Er^{3+}. The green and red upconversion emission of the samples was observed, and attributed to $^2H_{11/2}$, $^4S_{3/2} \rightarrow {}^4I_{15/2}$ and $^4F_{9/2} \rightarrow {}^4I_{15/2}$ transitions, respectively. The ratio of intensity of green emission to that of red emission was drastically changed with a change in EDTA 2Na concentration, which was mainly a result of different concentrations of EDTA 2Na leading to relatively different concentrations of Yb^{3+} ions in the nanoparticles. This affected the following energy transfer process of doping ions. The energy transfer process, $^4F_{7/2}$ $(Er) + {}^4F_{7/2}(Yb) \rightarrow {}^4I_{11/2}(Er) + {}^4F_{5/2}(Yb)$, depopulated the excited $^4F_{7/2}$ level and caused a decrease in green emission intensity. In addition, the increase in hychoxyl and carbonates of smaller crystallite size were also helpful to depopulate Er^{3+} ions in the $^2H_{11/2}$ and $^4S_{3/2}$ levels. This revealed that the upconversion processes in the nanoparticles depended on doping concentration and microstructure.

References:

[1] Dhanaraj J, Jagannathan R, Kutty T R N, Lu C H. Photoluminescence characteristics of Y_2O_3:Eu^{3+} nanophosphors prepared using sol-gel thermolysis. *J. Phys. Chem. B,* 2001, **105**: 11098.

[2] Kim Anh T, Quov Minh L, Vu N, Thu Huong T, Thanh Huong U, Barthal C, Strek W. Nanomaterials containing rare-earth ions Tb, Eu, Er and Yb: preparation, optical properties and application potential. *J. Lumin.*, 2003, **102-103**: 391.

[3] Wang LY, Li Y D. Na(Y$_{1.5}$Na$_{0.5}$)F$_6$ single-crystal nanorods as multicolor luminescent materials. *Nano Lett.*, 2006, **6**: 1645.

[4] Pei X J, Hong Y B, Zhao S L, Xu Z, Teng F. Frequency upconversion of Tm^{3+} and Yb^{3+} codoped YliF$_4$ synthesized by hydrothermal method. *Mater. Chem. Phys.*, 2005, **90**: 270.

[5] Sun Y, Liu H, Wang X, Kong X, Zhang H. Optical spectroscopy and Visible upconversion studies of YVO$_4$:Er^{3+} nanocrystals synthesized by a hydrothermal process. *Chem. Mater.*, 2006, **18**: 2726.

[6] Vetrone F, Boyer J C, Capobianco J A. Effect of Yb^{3+} codoping on the upconversion emission in nanocrystalline Y_2O_3: Er^{3+}. *J. Phys. Chem.*, 2003, **107**(5): 1107.

[7] Vetrone F, Boyer J C, Capobianco J A, Significance of Yb^{3+} concentration on the upconversion mechanisms in codoped Y_2O_3:Er^{3+},Yb^{3+} nanocrystals. *J. Appl. Phys.*, 2004, **96**: 661.

[8] Hirai T, Orikoshi T. Preparation of Gd$_2$O$_3$:Yb,Er and Gd$_2$O$_2$S: Yb, Er infrared to visible conversion phosphor ultradine particles using an emulsion liquid membrane system. *J. Colloid Interface. Sci.*, 2004, **69**:103.

[9] Pires A M, Serra O A. Low-temperature upconversion spectroscopy of nanosized Y_2O_3: Yb, Er phosphor. *J. Appl. Phys.*, 2005, **98**: 063529-1-: 063529-7.

[10] De G H, Qin W P, Zhang J S, Zhang J H, Wang Y, Cao C Y, Cui Y. Upconversion luminescence properties of d Y_2O_3: Yb^{3+}, Er^{3+} nanostructures. *J. Lumin.*, 2006, **119-120**: 258.

[11] Capobianco J A, Boyer J C, Vetrone F, Speghini A, Bettinelli M. Optical spectroscopy and upconversion studies of Ho^{3+}-doped bulk and nanocrystalline Y$_2$O$_3$. *Chem. Mater.*, 2002, **14**: 2915.

[12] Silver J, Maritinez-Rubio M I, Ireland T G, Fem G R, Withnall R. The effect of particle morphology and crystallite size on the upconversion luminescence properties of erbium and Ytterbium co-coded Yttrium oxide phosphors. *J. Phys. Chem. B*, 2001, **105**: 948.

[13] Ding Z S, Weng E J, Yang J. Application of chemical complexation approach in sol-gel process. *J. Chin. Cermic Soc.,*

1995, **23**(5): 571.

[14] Guo H, Dong N, Yin M, Zhang W, Lou L, Xia S. Visible upconversion in rare earth ion-doped Gd$_2$O$_3$ nanocrystals. *J. Phys. Chem. B*, 2004, **108**: 19205.

[15] Matsuura D. Red, green, and blue upconversion luminescence of trivalent-rare-earth ion- doped Y$_2$O$_3$ nanocrystals. *Appl. Phys. Lett.*, 2002, **81**(24): 4526.

[16] Li G, Sun B, Yang F, Chen D, Zhou Y, Cheng J. Synthesis and characterization of high-efficient nanocrystal up-conversion phosphors: ytterbium and erbium codoped lanthanum molybdate. *Chem. Mater.*, 2002, **14**: 2910.